

# Commonness and rarity in the marine biosphere

Sean R. Connolly<sup>a,1</sup>, M. Aaron MacNeil<sup>b</sup>, M. Julian Caley<sup>b</sup>, Nancy Knowlton<sup>c,1</sup>, Ed Cripps<sup>d</sup>, Mizue Hisano<sup>a</sup>, Loïc M. Thibaut<sup>a</sup>, Bhaskar D. Bhattacharya<sup>e</sup>, Lisandro Benedetti-Cecchi<sup>f</sup>, Russell E. Brainard<sup>g</sup>, Angelika Brandt<sup>h</sup>, Fabio Bulleri<sup>f</sup>, Kari E. Ellingsen<sup>i</sup>, Stefanie Kaiser<sup>j</sup>, Ingrid Kröncke<sup>k</sup>, Katrin Linse<sup>l</sup>, Elena Maggi<sup>f</sup>, Timothy D. O'Hara<sup>m</sup>, Laetitia Plaisance<sup>c</sup>, Gary C. B. Poore<sup>m</sup>, Santosh K. Sarkar<sup>e</sup>, Kamala K. Satpathy<sup>n</sup>, Ulrike Schückel<sup>k</sup>, Alan Williams<sup>o</sup>, and Robin S. Wilson<sup>m</sup>

<sup>a</sup>School of Marine and Tropical Biology, and Australian Research Council Centre of Excellence for Coral Reef Studies, James Cook University, Townsville, QLD 4811, Australia; <sup>b</sup>Australian Institute of Marine Science, Townsville, QLD 4810, Australia; <sup>c</sup>National Museum of Natural History, Smithsonian Institution, Washington, DC 20013; <sup>d</sup>School of Mathematics and Statistics, University of Western Australia, Perth, WA 6009, Australia; <sup>e</sup>Department of Marine Science, University of Calcutta, Calcutta 700 019, India; <sup>f</sup>Dipartimento di Biologia, University of Pisa, I-56126 Pisa, Italy; <sup>g</sup>Coral Reef Ecosystem Division, Pacific Islands Fisheries Science Center, National Oceanic and Atmospheric Administration, Honolulu, HI 96818; <sup>h</sup>Biocenter Grindel and Zoological Museum, University of Hamburg, 20146 Hamburg, Germany; <sup>i</sup>Norwegian Institute for Nature Research, FRAM—High North Research Centre for Climate and the Environment, 9296 Tromsø, Norway; <sup>j</sup>German Centre for Marine Biodiversity Research, Senckenberg am Meer, 26382 Wilhelmshaven, Germany; <sup>k</sup>Marine Research Department, Senckenberg am Meer, 26382 Wilhelmshaven, Germany; <sup>l</sup>British Antarctic Survey, Cambridge CB3 0ET, United Kingdom; <sup>m</sup>Museum Victoria, Melbourne, VIC 3001, Australia; <sup>n</sup>Environment and Safety Division, Indira Gandhi Centre for Atomic Research, Kalpakkam 603 102, India; and <sup>o</sup>Commonwealth Scientific and Industrial Research Organization, Marine and Atmospheric Research, Marine Laboratories, Hobart, TAS 7001, Australia

Contributed by Nancy Knowlton, April 28, 2014 (sent for review November 25, 2013; reviewed by Brian McGill and Fangliang He)

**Explaining patterns of commonness and rarity is fundamental for understanding and managing biodiversity. Consequently, a key test of biodiversity theory has been how well ecological models reproduce empirical distributions of species abundances. However, ecological models with very different assumptions can predict similar species abundance distributions, whereas models with similar assumptions may generate very different predictions. This complicates inferring processes driving community structure from model fits to data. Here, we use an approximation that captures common features of “neutral” biodiversity models—which assume ecological equivalence of species—to test whether neutrality is consistent with patterns of commonness and rarity in the marine biosphere. We do this by analyzing 1,185 species abundance distributions from 14 marine ecosystems ranging from intertidal habitats to abyssal depths, and from the tropics to polar regions. Neutrality performs substantially worse than a classical nonneutral alternative: empirical data consistently show greater heterogeneity of species abundances than expected under neutrality. Poor performance of neutral theory is driven by its consistent inability to capture the dominance of the communities' most-abundant species. Previous tests showing poor performance of a neutral model for a particular system often have been followed by controversy about whether an alternative formulation of neutral theory could explain the data after all. However, our approach focuses on common features of neutral models, revealing discrepancies with a broad range of empirical abundance distributions. These findings highlight the need for biodiversity theory in which ecological differences among species, such as niche differences and demographic trade-offs, play a central role.**

metacommunities | marine macroecology | species coexistence | Poisson-lognormal distribution

**D**etermining how biodiversity is maintained in ecological communities is a long-standing ecological problem. In species-poor communities, niche and demographic differences between species can often be estimated directly and used to infer the importance of alternative mechanisms of species coexistence (1–3). However, the “curse of dimensionality” prevents the application of such species-by-species approaches to high-diversity assemblages: the number of parameters in community dynamics models increases more rapidly than the amount of data, as species richness increases. Moreover, most species in high-diversity assemblages are very rare, further complicating the estimation of strengths of ecological interactions among species, or covariation in different species' responses to environmental fluctuations. Consequently, ecologists have focused instead on making assumptions about the overall distribution of demographic rates, niche

sizes, or other characteristics of an assemblage, and then deriving the aggregate assemblage properties implied by those assumptions (4–8). One of the most commonly investigated of these assemblage-level properties is the species abundance distribution (SAD)—the pattern of commonness and rarity among species (9–11). Ecologists have long sought to identify mechanisms that can explain common features of, and systematic differences among, the shapes of such distributions, and have used the ability to reproduce empirical SADs as a key test of biodiversity theory in species-rich systems (4, 6, 11–14).

Over the last decade, one of the most prevalent and influential approaches to explaining the structure of high-diversity assemblages has been neutral theory of biodiversity (12, 15, 16). Neutral models assume that individuals are demographically and ecologically equivalent, regardless of species. Thus, variation in relative

## Significance

Tests of biodiversity theory have been controversial partly because alternative formulations of the same theory seemingly yield different conclusions. This has been a particular challenge for neutral theory, which has dominated tests of biodiversity theory over the last decade. Neutral theory attributes differences in species abundances to chance variation in individuals' fates, rather than differences in species traits. By identifying common features of different neutral models, we conduct a uniquely robust test of neutral theory across a global dataset of marine assemblages. Consistently, abundances vary more among species than neutral theory predicts, challenging the hypothesis that community dynamics are approximately neutral, and implicating species differences as a key driver of community structure in nature.

Author contributions: S.R.C., M.A.M., and M.J.C. designed research; N.K., B.D.B., L.B.-C., R.E.B., A.B., F.B., K.E.E., S.K., I.K., K.L., E.M., T.D.O., L.P., G.C.B.P., S.K.S., K.K.S., U.S., A.W., and R.S.W. performed research; S.R.C., E.C., M.H., and L.M.T. analyzed data; S.R.C. designed analytical approach; M.J.C. initiated the collaboration between Census of Marine Life and S.R.C.; N.K. was the initiator of Census of Marine Life Project (producer of dataset) for coral reefs; N.K. designed data collection protocols; B.D.B., L.B.-C., R.E.B., A.B., F.B., K.E.E., S.K., I.K., K.L., E.M., T.D.O., L.P., G.C.B.P., S.K.S., K.K.S., U.S., A.W., and R.S.W. provided advice on treatment of data for analyses; and S.R.C., M.A.M., M.J.C., N.K., and E.C. wrote the paper.

Reviewers: B.M., University of Maine; F.H., University of Alberta.

The authors declare no conflict of interest.

Freely available online through the PNAS open access option.

<sup>1</sup>To whom correspondence may be addressed. E-mail: knowlton@si.edu or Sean.connolly@jcu.edu.au.

This article contains supporting information online at [www.pnas.org/lookup/suppl/doi:10.1073/pnas.1406664111/-DCSupplemental](http://www.pnas.org/lookup/suppl/doi:10.1073/pnas.1406664111/-DCSupplemental).



idiosyncratic ways, or whether there are particular features of real SADs that cannot be captured by neutral models.

## Results

A gamma distribution of species abundances closely approximates several alternative neutral models across a broad range of neutral model parameter values (Fig. S1; see *SI Results* for further discussion). Moreover, the gamma consistently outperforms the lognormal when fitted to data simulated from neutral models. Specifically, as the number of distinct species abundance values in the simulated data increases, the relative support for the gamma distribution becomes consistently stronger for all of the neutral models we considered (Fig. 2A). This reflects the fact that datasets with only a small number of abundance values (e.g., a site containing 11 species, 10 of which are only represented by one individual) provide very little information about the shape of the SAD, whereas those with more abundance values provide more information (e.g., a site with 100 species whose abundances are spread over 10–20 different values).

In contrast to their relative fit to simulated neutral SADs, the lognormal consistently outperforms the gamma distribution when fitted to real marine species abundance data. When considered in terms of average support per SAD, relative support for the lognormal becomes consistently stronger as the number of observed species abundance values increases, in direct contrast with the simulated neutral data (Fig. 2B). Moreover, when the strength of evidence is considered cumulatively across all sites for each dataset, the lognormal has well over 99% support as the better model in each case (Table 1). This substantially better fit of the lognormal is retained in every case when data are pooled to the mesoscale, and, in all cases save one, when data are pooled at the regional scale (Table 1, Fig. 2B, and Figs. S2 and S3). The lognormal also remained strongly favored when we tested the robustness of our results by classifying species into taxonomic and ecological guilds, and restricting our analysis to the most species-rich guild within each dataset (see *SI Results* and Table S3).

Inspection of the lack of fit of the gamma neutral approximation indicates that it deviates from the data in highly consistent ways: real SADs exhibit substantially more heterogeneity than the gamma distribution can generate (Fig. 3). Specifically, the gamma is unable to simultaneously capture the large number of rare species and the very high abundances of the most common

species. For abundance distributions lacking an internal mode (i.e., where the leftmost bar in the SAD is the largest one), this is manifested as an excess of rare species and paucity of species with intermediate abundance, relative to the best-fit neutral approximation (Fig. 3A, blue lines). Conversely, when an internal mode is present in the data, the abundances of the most highly abundant species are consistently higher than the gamma distribution can produce (Fig. 3B, blue lines). In contrast, discrepancies between the data and the lognormal are much smaller in magnitude, and more symmetrically distributed around zero, compared with the gamma (Fig. 3, red lines).

Detailed analysis of variation in the strength of evidence against neutrality, within and among datasets, indicates that the relative performance of the lognormal over the gamma is substantially driven by the fact that the most abundant species is, on average, too dominant to be captured by the gamma neutral approximation. After controlling for the effects of the number of abundance values in the sample on statistical power, the relative abundance of the most-abundant species explained over one-half of the variation in the strength of support for the lognormal over the gamma, for site-level, mesoscale, and regional-scale abundance distributions (Table S4, Fig. S4, and *SI Results*). Conversely, the prevalence of rarity was a poor predictor of the strength of evidence against the gamma neutral approximation (Table S4, Fig. S5, and *SI Results*).

In addition to outperforming the gamma neutral approximation, tests of the absolute goodness of fit of the lognormal suggest that it approximates the observed species abundance data well. Statistically significant lack of fit (at  $\alpha = 0.05$ ) to the lognormal was detected in 4.8% of sites, approximately equal to what would be expected by chance, under the null hypothesis that the SADs are in fact lognormal. Moreover, lognormal-based estimates of the number of unobserved species in the regional species pool are realistic, and very similar to those produced by an alternative, nonparametric jackknife method that relies on presence–absence rather than abundance data (Fig. 4).

## Discussion

Recently, the use of SADs to test biodiversity theory has been criticized because different species abundance models often generate very similar predictions, which can be difficult to distinguish when fitted to species abundance data (9). Consequently, some researchers have focused on other properties of assemblages, such as community similarity (12), species–area and species–time relationships (23, 24), and relationships between species traits or phylogeny and species abundance (25, 26). Such approaches are powerful when evaluating the performance of particular species abundance models. However, because models combine multiple assumptions, attributing a model's failure to one assumption in particular, such as species equivalence, is problematic. Indeed, in the debate over neutral theory of biodiversity, studies that show failure of a neutral model (12, 25, 27) are almost invariably followed by responses showing that packaging neutrality with a different set of alternative assumptions can explain the data after all (11, 28, 29). Although the identification of alternative auxiliary assumptions that preserve a theory's core prevents premature abandonment of a promising theory, it also can hinder progress by inhibiting the reallocation of scientific effort to more promising research programs (30). Given the proliferation of alternative theories of biodiversity (8, 14, 31, 32), identifying and testing predictions that are robust to auxiliary assumptions, and therefore better target a theory's core assumptions, should be a high priority.

Here, we showed that, as previously hypothesized (22), a gamma distribution successfully captures features common to several models that share the core neutrality assumptions of species equivalence, but make very different auxiliary assumptions. We then found that this approximation cannot simultaneously

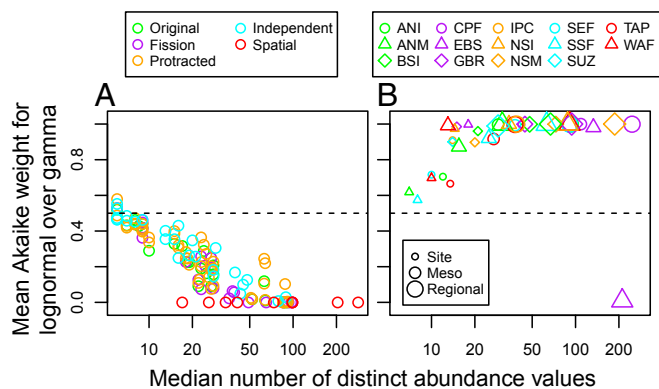


**Fig. 2.** Species abundances are better approximated by (A) a gamma distribution for simulated neutral communities, but (B) a lognormal distribution for the empirical data. Percentage support for the lognormal versus the gamma is plotted as a function of the number of observed distinct species abundances. In A, different neutral models are plotted with different colors, and each point represents a particular neutral model parameter combination from Fig. S1. In B, each combination of symbol and color represents a different marine ecosystem, whereas increasing symbol size indicates the increasing scale at which abundances were pooled (site, mesoscale, and regional).



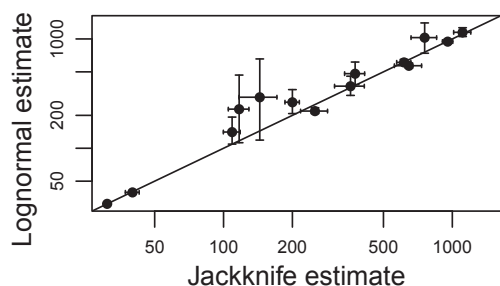


**Fig. 4.** Agreement between lognormal-based and nonparametric estimates of the total number of species in the community. Points on the horizontal axis are richness estimates produced by the nonparametric jackknife, based on presence–absence data across sites. The points on the vertical axis are estimates produced by the lognormal model, fitted to the pooled regional abundance distributions. Error bars are 95% confidence intervals. The solid line is the unity line, where the lognormal and the nonparametric jackknife produce the same estimate of the number of unobserved species.

## Conclusions

Neutral theory explains variation in the abundances and distribution of species entirely as a consequence of demographic stochasticity—chance variation in the fates of individuals (15, 36). Although proponents of neutral theory have always acknowledged the existence of ecological differences between species, neutral theory assumes that those differences are overwhelmed by the phenomena that are explicitly included in neutral models (14, 36). The formulation and testing of neutral theory has drawn attention to the potential importance of demographic stochasticity as a process that contributes to differences in species abundances that are unrelated to species' ecological traits, such as niche size or competitive ability. Such effects should be particularly important among rare species (4). Indeed, our finding that there are common features of different neutral models suggests that it can play a role as a robust null expectation, at least for some aspects of community structure (16). However, the most abundant few species often numerically dominate communities and play a disproportionately large role in community and ecosystem processes (37). We have shown that neutral theory consistently underestimates among-species heterogeneity in abundances across a broad range of marine systems. The fact that its performance is closely linked to abundances of the most common species indicates that it is the ecological dominance of these very highly abundant species that cannot be explained by neutral processes alone. Commonness itself is poorly understood, but the identities of the most common species in ecosystems tend to remain quite consistent over ecological timescales (38). Thus, the key to understanding the distribution of abundances in communities, even species-rich ones, may lie as much in understanding how the characteristics of common species allow them to remain so abundant, as in understanding the dynamics and persistence of rare species.

## Materials and Methods

**Approximating Neutrality.** Pueyo's framework starts with a stochastic differential equation for random drift in population size (i.e., birth rate equals death rate, no density dependence, immigration, emigration, or speciation) and considers approximating departures from this model in terms of successively higher-order perturbations to it. Here, we take as our candidate neutral approximation the gamma distribution and, as our alternative model, the lognormal distribution. More specifically, because species abundance data are discrete, whereas the gamma and lognormal are continuous distributions, we use the Poisson-gamma (i.e., negative binomial) and Poisson-lognormal mixture distributions, as these distributions are commonly used to approximate discrete, random samples from underlying gamma or lognormal community abundance distributions (see *SI Materials and Methods* for further details).

To assess whether the Poisson-gamma distribution provides a good approximation to the SADs produced under neutrality, we tested it against five

different neutral models: Hubbell's original neutral model (39), a protracted speciation neutral model (21), a fission speciation model (40), an independent species model (11, 41), and a spatially explicit neutral model (42). We chose these five models because they encompass models that relax key assumptions of neutral theory as originally formulated; moreover, each of them meets a strict definition of neutrality: every individual has the same demographic rates, and the same per-capita effects on other individuals, regardless of species. We tested the approximation in two ways. First, we assess how closely (in absolute terms) the Poisson-gamma can approximate neutral abundance distributions. Second, we assess whether the Poisson-gamma outperforms the Poisson-lognormal when fitted to data generated according to neutral model assumptions (see *SI Materials and Methods* for details).

**Empirical Data.** Data were contributed to the Census of Marine Life (CoML) project and represent a diverse range of taxa, ocean realms, depths, and geographic locations (Table S1). To be included in our analysis, contributed data needed to meet several criteria (see *SI Materials and Methods* for details). Where datasets included samples over multiple years from the same sites, only the most recent year of data was used. Finally, we only fitted SADs if they contained more than five distinct species abundance values, to minimize convergence problems associated with fitting species abundance models to very sparse data. However, the data from such sites were still used in the analyses that pooled abundance distributions at larger scales.

**Fitting Models to Species Abundance Data.** For both the simulated neutral data, and the real species abundance data, we fitted our models using maximum-likelihood methods (see *SI Materials and Methods* for details). For the empirical data, in addition to fitting our species abundance models at the site level, we also fitted pooled species abundances at a mesoscale level, and at the regional (whole-dataset) level. For datasets that were spatially hierarchically organized, we used this hierarchy to determine how to pool sites at the mesoscale [e.g., for the Central Pacific Reef Fish (CPF) data, sites were nested within islands, so pooling was done to the island level]. For data that were not explicitly hierarchically organized [Antarctic Isopods (ANI), Antarctic Molluscs (ANM), Scotian Shelf Fish (SSF), Bass Strait Intertidal (BSI)], cluster analysis was used to identify mesoscale-level groupings. In two cases [Sunderban Zooplankton (SUZ), Indo-Pacific Coral Crustaceans (IPC)], there were only a few sites sampled, and no natural hierarchical structure, so these data were omitted from the mesoscale analysis.

For both the analysis of the marine species abundance data, and the analysis of the simulated neutral communities, model selection was based on Akaike weights, which are calculated from Akaike's information criterion values and estimate the probability (expressed on a scale of 0–1) that a model is actually the best approximating model in the set being considered. Because the Poisson-gamma and the Poisson-lognormal have the same number of estimated parameters, this is equivalent to calculating model weights based on the Bayesian information criterion. For the empirical data, model selection was done at the whole-dataset level by summing the log-likelihoods for all individual sites (for the site-level analysis) or mesoscale (for the mesoscale analysis) abundance distributions for a dataset, and calculating Akaike weights based on these values (Table 1). However, this approach does not make sense for the analysis of the simulated neutral SADs, because an arbitrary degree of confidence can be obtained by simulating a large number of sites. Therefore, we instead calculated an expected level of model support on a per-SAD basis, for each neutral model and parameter combination, by calculating the mean difference in log-likelihoods across the 100 simulated datasets, and converting this mean into an Akaike weight. We examined these Akaike weights as functions of the number of distinct observed species abundance values, because we would expect our ability to distinguish between alternative models to increase as the number of distinct observed species abundance values increases. For comparison, we also calculated per-SAD Akaike weights for the marine species abundance data. This approach is less powerful than the aggregate whole-dataset comparisons shown in Table 1, but it facilitates visualization of the differences between the simulated neutral SADs (Fig. 2A) and the real marine SADs (Fig. 2B).

**Analysis of Variation in Performance of Neutral Approximation.** The discrepancies between the data and the gamma neutral approximation suggest that real data exhibit too much heterogeneity in species' abundances to be captured by the neutral approximation. To better understand this, we examined whether the relative model support varied systematically within or among datasets as a function of the prevalence of rare species, and the abundances of the most abundant species. As a measure of relative model support, we used a per-observation difference in log-likelihoods (see *SI Materials and Methods* for details). We first confirmed that this standardization

controlled for the effect of sample size on statistical power (i.e., the trend illustrated in Fig. 2B). Then, we asked whether the variation in standardized model support was better explained by the numerical dominance of the most common species, or by the prevalence of very rare species, using mixed-effects linear models.

**Testing the Absolute Fit of the Lognormal Distribution.** Goodness of fit of the lognormal distribution to the empirical data was assessed with parametric bootstrapping (see *SI Materials and Methods* for details). Also, for each dataset's regional-scale SAD, we compared lognormal-based estimates of total number of species in the species pool with estimates using the non-parametric jackknife (10). See *SI Materials and Methods* for further details.

**ACKNOWLEDGMENTS.** U.S. acknowledges S. Ehrich and A. Sell for providing ship time. The authors thank all participants in the Census of Marine Life

project, particularly S. Campana, M. Sogin, K. Stocks, and L. A. Zettler. They also thank R. Etienne for providing advice for obtaining numerical solutions of the fission speciation neutral model, and J. Rosindell and S. Cornell for sharing simulated neutral community data from their spatially explicit neutral model. The authors thank T. Hughes for comments on an early version of the manuscript. K.E.E. acknowledges The Norwegian Oil and Gas Association for permitting use of data. A.B. acknowledges the support of the Ministry for Science and Technology and the German Research Foundation (Deutsche Forschungsgemeinschaft) for support of the Antarctic benthic deep-sea biodiversity (ANDEEP) and ANDEEP-System Coupling (SYSTCO) expeditions, as well as five PhD positions. A.B. also thanks the Alfred-Wegener-Institute for Polar and Marine Research for logistic help, as well as the crew of the vessel and all pickers, sorters and identifiers of the extensive deep-sea material. The Census of Marine Life funded the assembly of the metadataset. Analysis of the data was made possible by funding from the Australian Research Council (to S.R.C.).

- Angert AL, Huxman TE, Chesson P, Venable DL (2009) Functional tradeoffs determine species coexistence via the storage effect. *Proc Natl Acad Sci USA* 106(28):11641–11645.
- Levine JM, HilleRisLambers J (2009) The importance of niches for the maintenance of species diversity. *Nature* 461(7261):254–257.
- Adler PB, Ellner SP, Levine JM (2010) Coexistence of perennial plants: An embarrassment of niches. *Ecol Lett* 13(8):1019–1029.
- Sæther BE, Engen S, Grøtan V (2013) Species diversity and community similarity in fluctuating environments: Parametric approaches using species abundance distributions. *J Anim Ecol* 82(4):721–738.
- Scheffer M, van Nes EH (2006) Self-organized similarity, the evolutionary emergence of groups of similar species. *Proc Natl Acad Sci USA* 103(16):6230–6235.
- MacArthur JW (1960) On the relative abundance of species. *Am Nat* 94(874):25–34.
- Clark JS (2010) Individuals and the variation needed for high species diversity in forest trees. *Science* 327(5969):1129–1132.
- Tokeshi M (1999) *Species Coexistence: Ecological and Evolutionary Perspectives* (Blackwell Science, Oxford).
- McGill BJ, et al. (2007) Species abundance distributions: Moving beyond single prediction theories to integration within an ecological framework. *Ecol Lett* 10(10):995–1015.
- Connolly SR, Hughes TP, Bellwood DR, Karlson RH (2005) Community structure of corals and reef fishes at multiple scales. *Science* 309(5739):1363–1365.
- Volkov I, Banavar JR, Hubbell SP, Maritan A (2007) Patterns of relative species abundance in rainforests and coral reefs. *Nature* 450(7166):45–49.
- Dornelas M, Connolly SR, Hughes TP (2006) Coral reef diversity refutes the neutral theory of biodiversity. *Nature* 440(7080):80–82.
- May RM (1975) *Ecology and Evolution of Communities*, eds Cody ML, Diamond JM (Belknap Press of Harvard Univ Press, Cambridge, MA), pp 81–120.
- Hubbell SP (2001) *The Unified Neutral Theory of Biodiversity and Biogeography* (Princeton Univ Press, Princeton).
- Clark JS (2009) Beyond neutral science. *Trends Ecol Evol* 24(1):8–15.
- Rosindell J, Hubbell SP, He FL, Harmon LJ, Etienne RS (2012) The case for ecological neutral theory. *Trends Ecol Evol* 27(4):203–208.
- McGill BJ (2003) A test of the unified neutral theory of biodiversity. *Nature* 422(6934):881–885.
- Connolly SR, Dornelas M, Bellwood DR, Hughes TP (2009) Testing species abundance models: A new bootstrap approach applied to Indo-Pacific coral reefs. *Ecology* 90(11):3138–3149.
- Etienne RS, Olff H (2005) Confronting different models of community structure to species-abundance data: A Bayesian model comparison. *Ecol Lett* 8(5):493–504.
- Muneepeerakul R, et al. (2008) Neutral metacommunity models predict fish diversity patterns in Mississippi-Missouri basin. *Nature* 453(7192):220–222.
- Rosindell J, Cornell SJ, Hubbell SP, Etienne RS (2010) Protracted speciation revitalizes the neutral theory of biodiversity. *Ecol Lett* 13(6):716–727.
- Pueyo S (2006) Diversity: Between neutrality and structure. *Oikos* 112(2):392–405.
- Adler PB (2004) Neutral models fail to reproduce observed species-area and species-time relationships in Kansas grasslands. *Ecology* 85(5):1265–1272.
- McGill BJ, Hadly EA, Maurer BA (2005) Community inertia of Quaternary small mammal assemblages in North America. *Proc Natl Acad Sci USA* 102(46):16701–16706.
- Ricklefs RE, Renner SS (2012) Global correlations in tropical tree species richness and abundance reject neutrality. *Science* 335(6067):464–467.
- Bode M, Connolly SR, Pandolfi JM (2012) Species differences drive nonneutral structure in Pleistocene coral communities. *Am Nat* 180(5):577–588.
- Wills C, et al. (2006) Nonrandom processes maintain diversity in tropical forests. *Science* 311(5760):527–531.
- Lin K, Zhang DY, He FL (2009) Demographic trade-offs in a neutral model explain death-rate—abundance-rank relationship. *Ecology* 90(11):31–38.
- Chen AP, Wang SP, Pacala SW (2012) Comment on “Global correlations in tropical tree species richness and abundance reject neutrality” *Science* 336(6089):1639, author reply 1639.
- Lakatos I (1978) *The Methodology of Scientific Research Programmes* (Cambridge Univ Press, Cambridge, UK).
- McGill BJ (2010) Towards a unification of unified theories of biodiversity. *Ecol Lett* 13(5):627–642.
- Harte J (2011) *Maximum Entropy and Ecology: A Theory of Abundance, Distribution, and Energetics* (Oxford Univ Press, Oxford).
- Engen S, Lande R (1996) Population dynamic models generating the lognormal species abundance distribution. *Math Biosci* 132(2):169–183.
- Sugihara G, Bersier LF, Southwood TRE, Pimm SL, May RM (2003) Predicted correspondence between species abundances and dendrograms of niche similarities. *Proc Natl Acad Sci USA* 100(9):5246–5251.
- Engen S, Lande R, Walla T, DeVries PJ (2002) Analyzing spatial structure of communities using the two-dimensional poisson lognormal species abundance model. *Am Nat* 160(1):60–73.
- Alonso D, Etienne RS, McKane AJ (2006) The merits of neutral theory. *Trends Ecol Evol* 21(8):451–457.
- Gaston KJ (2010) Ecology. Valuing common species. *Science* 327(5962):154–155.
- Gaston KJ (2011) Common ecology. *Bioscience* 61(5):354–362.
- Etienne RS, Alonso D (2005) A dispersal-limited sampling theory for species and alleles. *Ecol Lett* 8(11):1147–1156.
- Etienne R, Haegeman B (2011) The neutral theory of biodiversity with random fission speciation. *Theor Ecol* 4(1):87–109.
- He F (2005) Deriving a neutral model of species abundance from fundamental mechanisms of population dynamics. *Funct Ecol* 19(1):187–193.
- Rosindell J, Cornell SJ (2013) Universal scaling of species-abundance distributions across multiple scales. *Oikos* 122(7):1101–1111.

# Supporting Information

Connolly et al. 10.1073/pnas.1406664111

## SI Text

### SI Materials and Methods

**Candidate Neutral and Nonneutral Approximations.** A set of non-interacting populations undergoing pure random drift in population size (birth rate equals death rate, no immigration, emigration, or environmental stochasticity) produces a species abundance distribution in which the probability that a species has a given abundance,  $n$ , varies inversely with abundance (1). On log-log scale, this is a straight line with a slope of  $-1$ :

$$\log(f(n)) = \log(\kappa) - \log(n), \quad [\text{S1}]$$

where  $f(n)$  is the probability that a species has abundance  $n$ , and  $\kappa$  is a normalizing constant. Neutral models have two characteristics that cause them to depart from the case of pure random drift. First, because species are ecologically identical, there is a constraint on total community size that is independent of species richness. Using a maximum entropy argument, a modification to this power-law model can be derived that accounts for this constraint (1):

$$\log(f(n)) = \log(\kappa) - \log(n) - \phi n. \quad [\text{S2}]$$

Eq. S2 is equivalent to Fisher's log-series distribution (1). Second, neutral models also may have characteristics that cause individual species' dynamics to depart from the pure drift assumption, such as dispersal limitation (2), or unequal birth and death rates (3). Pueyo (1) conceptualizes small departures from pure drift as perturbations to the value of the slope of  $-1$  in Eq. S1. The combination of these two extensions to Eq. S1 yields the following:

$$\log(f(n)) = \log(\kappa) - \beta \log(n) - \phi n. \quad [\text{S3}]$$

Note that, by setting  $\beta = 1 - k$  and  $\phi = 1/a$ , and the normalization constant  $\kappa = (\Gamma(k)a^k)^{-1}$ , it becomes apparent that  $f(n)$  in Eq. S3 is a gamma distribution with shape  $k$  and scale  $a$ . Because it is well known that many neutral models can depart markedly from the log-series distribution (2, 4, 5), we take the gamma distribution as our candidate neutral approximation.

Increasingly large departures from neutrality might be poorly approximated by a perturbation to the slope of a power-law relationship, in which case a second-order perturbation may be needed, where a quadratic term is added to the first-order model:

$$\log(f(n)) = \log(\kappa) - \beta \log(n) + c [\log(n)]^2. \quad [\text{S4}]$$

If we set  $\beta = 1 - \mu/\sigma^2$ ,  $c = -1/(2\sigma^2)$ , and  $\log(\kappa) = -(\frac{\mu^2}{2\sigma^2} + \log(\sqrt{2\pi}\sigma))$ , then  $f(n)$  in Eq. S4 is a lognormal distribution where  $\mu$  and  $\sigma$  are the mean and SD of  $\log(n)$ , respectively (1). We therefore take the lognormal as our candidate nonneutral approximation.

Because the gamma and lognormal distributions are continuous, whereas abundances are integer-valued, and because many species abundance data are incomplete samples from an underlying community abundance distribution, in our analyses we assess our neutral and nonneutral approximations by fitting Poisson-gamma (i.e., negative binomial) and Poisson-lognormal mixture distributions:

$$P(r) = \int_{\lambda=0}^{\infty} \frac{\lambda^r e^{-\lambda}}{r!} f(\lambda) d\lambda, \quad [\text{S5}]$$

where  $P(r)$  is the probability that a species has abundance  $r$  in the sample,  $\lambda$  is the mean of the Poisson distribution (and thus integrated out of the likelihood), and  $f(\lambda)$  is either the lognormal or the gamma distribution. These distributions are commonly used to represent random samples of individuals from underlying gamma or lognormal community abundance distributions, respectively (6–8). More specifically, we use the zero-truncated forms of the Poisson-gamma and Poisson-lognormal distributions, because, by definition, a species is not observed in the sample if it has zero abundance (6):

$$p(r) = \frac{P(r)}{1 - P(0)}. \quad [\text{S6}]$$

**Assessing the Neutral Approximation.** Our five candidate neutral models exhibited a broad range of auxiliary assumptions. In Hubbell's "original neutral model," local communities are partially isolated by dispersal from the broader metacommunity, and new species arise with a fixed probability from individual birth events (analogous to mutation events in population-genetic neutral models) (9). The "protracted speciation neutral model" is similar to the original neutral model, but it incorporates a time lag between the appearance of an incipient new lineage, and its recognition as a distinct species (10). In the "fission speciation model," speciation occurs by random division of existing species (e.g., via vicariance); this model can exhibit a more superficially lognormal-like species abundance pattern than point speciation models, in that its log-abundance distributions are more symmetric about a single mode than other neutral models (5). In the "independent species model" (3, 11), population dynamics are density independent, per-capita birth rate is less than per-capita death rate, and there is a constant immigration rate. Finally, in the spatially explicit neutral model (4), speciation follows a point-mutation process (as in the original neutral model), and dispersal distances follow a Gaussian kernel. The first four models have explicit mathematical expressions for the species abundance distribution at equilibrium, which facilitates formally evaluating the neutral approximation: see equations below). For the spatially explicit neutral model, we used the approximate species abundance distributions generated by simulation in the original paper and kindly provided by the authors (4).

As noted in the main text, the strict definition of neutrality that applies to these models contrasts with symmetric models that implicitly allow for niche or demographic differences among species, for instance, by having within-species competition be stronger than between species competition (12), by implicitly including temporal niche differentiation via different responses to environmental fluctuations (13), or by allowing species with different life history types to differ in their speciation rates (14).

To assess how well the Poisson-gamma distribution approximates our alternative neutral models, we considered a broad range of neutral model parameter space spanning most of the realistic range for real species abundance data (hundreds to tens of thousands of individuals, and from less than 10 to many hundreds of species). For each neutral model parameter combination, we used the Kullback–Leibler (K-L) divergence, a measure of the information lost when one distribution is used as an approximation for another (15). Specifically, we found the Poisson-gamma distribution parameters that minimized the K-L divergence. For discrete data, such as counts, K-L divergence is as follows:

$$D = \sum_n \pi(n) \log\left(\frac{\pi(n)}{p(n)}\right), \quad [S7]$$

where  $n$  indexes the possible values of the random variable (in this case, abundance),  $\pi(n)$  is the distribution being approximated (the relevant neutral model), and  $p(n)$  is the approximating model—in this case, the zero-truncated Poisson-gamma distribution (Eq. S6).

Because our analysis of the empirical data is largely a comparative assessment of the Poisson-gamma and Poisson-lognormal distributions, our conclusions rely on an implicit assumption that a Poisson-gamma distribution would outperform a Poisson-lognormal if data were actually generated by neutral dynamics. Therefore, in addition to assessing the performance of the Poisson-gamma as a neutral approximation in absolute terms, we also simulated 100 species abundance distributions from each of the 126 equilibrium neutral abundance distributions used in the previous analysis (Fig. S1), and we compared the best-fit Poisson-gamma and Poisson-lognormal distributions for the 12,600 simulated abundance distributions, exactly as we did for the empirical species abundance distributions.

**Criteria for Empirical Data Inclusion.** Our criteria for data inclusion were as follows. First, the data needed to record counts of individual organisms for a given level of sampling effort (e.g., sample volume, or transect area). Second, data needed to be collected by experts (i.e., survey programs including data collected by amateurs were excluded), to minimize the risks of misidentification or miscounting. Third, data needed to be focused on the assemblage level, rather than on specific target species. Fourth, if sampling effort varied within species abundance samples, it had to be possible to standardize to a common level of effort. For instance, if fishes were counted on 10-m<sup>2</sup> and 50-m<sup>2</sup> transects, then 10/50 = 20% of the individuals on the larger transects were subsampled and pooled with the counts from the smaller transects (16). Three of the datasets we used required subsampling [Great Barrier Reef Fish (GBR), National Oceanic and Atmospheric Administration (NOAA) Central Pacific Reef Fish (CPF), and South East Fishery: Shelf Fish (SEF)].

**Model Fitting.** To assess the relative performance of the Poisson-gamma and Poisson-lognormal for both simulated neutral and real species abundance data, we found the gamma or neutral model parameters that maximized the log-likelihood for the zero-truncated forms of the Poisson-gamma and Poisson-lognormal abundance distributions:

$$\mathcal{L} = \sum_r n_r \log(p(r)), \quad [S8]$$

where  $n_r$  is the number of species with abundance  $r$  in the sample, and  $p(r)$  is the zero-truncated probability that a species has abundance  $r$  (Eq. S6). Best-fit models were obtained by finding the gamma or neutral model parameters that maximized the log-likelihood for each site.

**Analysis of Variation in the Shapes of Species Abundance Distributions.** To determine whether there was any systematic variation in the strength of evidence for gamma-like versus lognormal-like distributions, and whether any such variation was associated with systematic differences in the patterns of commonness and rarity in communities, we needed a sample-standardized measure of the relative strength of support for a candidate model. Specifically, the maximum log-likelihood for a species abundance model at a given site is the sum of the contributions of each species' abundance value to the log-likelihood. To control for this effect of the number of observations, we computed, for each site, a per-observation average

log-likelihood: the site's maximum log-likelihood divided by the number of species abundances contributing to that log-likelihood. This approach is used in time series analysis, when models that have been fitted to different numbers of observations (e.g., models with different time lags) must be compared (17). Our standardized measure of model support was simply the difference between the standardized gamma and lognormal maximum log-likelihoods.

As our measure of the dominance of common species, we took, in the first instance, the abundance of the most abundant species, expressed as a proportion of the total number of individuals in the species abundance distribution. As our rarity measure, we took the proportion of species that were singletons (i.e., represented by a single individual in the abundance distribution). We used linear mixed-effects models to characterize the extent to which these two quantities explained variation within and among datasets in the standardized support for the lognormal over the gamma, at all scales (site, mesoscale, regional). To confirm that our results were not sensitive to the particular commonness or rarity metrics we considered, we repeated our analysis using the combined abundance of the three most abundant species, and using the proportion of species in the bottom two octaves of abundance (i.e., with proportion of species with abundance three or less).

**Parametric Bootstrap Goodness of Fit.** Goodness of fit to the empirical data was assessed with parametric bootstrapping, using a hypergeometric algorithm described in detail elsewhere (7). Parametric bootstrapping involves simulating datasets that conform to the assumptions of a particular fitted species abundance model. For example, to test the goodness of fit of the Poisson-lognormal, one simulates Poisson random sampling of individuals from an underlying lognormal distribution of species abundances. Then, the model is fitted to each simulated dataset, and a goodness of fit statistic calculated. The frequency distribution of this statistic across simulated datasets approximates the statistic's expected distribution, under the null hypothesis that the data conform to the model. As a goodness of fit statistic, we use a normalized measure of model deviance, which, following convention, we term  $\hat{c}$  (16). Deviance is a likelihood-based measure of how far away the model is from exhibiting a perfect fit to the data.  $\hat{c}$  is obtained by taking all deviances for the model's fits to the observed and simulated data, and dividing each by the average of the simulated deviances. Thus,  $\hat{c}$  has an expected value of 1.0. We judged the lack of fit as statistically significant if the  $\hat{c}$  of the observed data was greater than 95% of the corresponding simulated  $\hat{c}$  values.

**Species Pool Estimation.** Using the maximum-likelihood estimates, the probability that a species is present in the species pool but has abundance zero in the sample,  $P(0)$ , is calculated from Eq. S5, by substituting 0 for  $r$ . Then, the number of species in the community that has been sampled can be estimated from the following:

$$\hat{S} = \frac{S_{obs}}{1 - P(0)}, \quad [S9]$$

where  $\hat{S}$  is the estimated number of species in the community, and  $S_{obs}$  is the number of species observed in the data. Non-parametric jackknife estimates were calculated using the frequency distribution of species occurrences across sites (i.e., presence-absence data: see ref. 16). Jackknife order was calculated separately for each dataset, using the sequential testing procedure recommended by ref. 18.

## SI Results

**Performance of the Neutral Approximation.** Fig. S1 depicts the fit of the neutral approximation to our five alternative neutral models. For the first three models, these plots encompass three order-of-magnitude variation in local community sizes,  $J$  ( $10^2$  to  $10^4$  in-

dividuals), because most species abundance distributions are on the order of hundreds to (occasionally) tens of thousands of individuals. Similarly, we show a broad range of immigration rates from  $m = 0.01$  (1% of newborns are immigrants) to 1.0 (an entirely open local community). We plot a range of values of the biodiversity parameter,  $\theta$ , so that the expected number of species in the community spanned a very broad range (typically from a low of about five species, for small, isolated communities with low  $\theta$ , to many hundreds of species for large, high-immigration communities with large  $\theta$ ). Note that the range of values of  $\theta$  needed to span these richness values differs between the fission speciation model and the first two models, because the parameter is defined somewhat differently in this model. The protracted speciation model includes an additional parameter,  $\tau'$ , which is the number of generations required for speciation to occur, relative to the metacommunity size (the special case  $\tau' = 0$  corresponds to the original neutral model). The fourth (independent species) neutral model differs from the others in that it does not explicitly characterize dynamics at the metacommunity scale. Rather, it implicitly assumes that species have equal abundance in the metacommunity (and thus they all have the same rate of immigration to the local community,  $\gamma$ ), and that species' local population dynamics are independent of one another, and thus a function of only  $\gamma$  and the ratio of local per-capita birth to death rates,  $x$ . Because within-species dynamics are also density independent, this is consistent with the neutrality assumption (individuals have no effect on one another's per-capita growth rates, regardless of whether they belong to the same or different species). This density-independent assumption means that the model is a probability distribution of species abundances, and not a model of overall species frequencies. Consequently, unlike the previous neutral models, it does not predict species richness. Similarly, for the spatially explicit model, the form of the species abundance distribution depends on the speciation probability ( $\nu$ ), and the ratio of the sampling area  $A$  (i.e., the local community size) to the squared width of the dispersal kernel,  $L$ , rather than either of the latter two variables independently (4). Thus, a given shape for the species abundance distribution can correspond to a broad range of different community species richness values, depending on whether  $A$  and  $L$  are both small or both large.

Fig. S1 shows that the Poisson-gamma neutral approximation performs very well in the overwhelming majority of cases. There are, however, some cases where the approximation performs less well. These typically correspond to parameter combinations that imply very species-poor assemblages. One class of such cases corresponds to small ( $\sim 100$  individuals), very low-immigration, low-diversity assemblages ( $\sim 5$  species; e.g., *Top Left* of Fig. S1A). Here, the neutral model has an elevated probability that one species is nearly monodominant (the curve bends upward at the right, for species abundances close to the total community size), which the Poisson-gamma distribution cannot capture. A second class of cases, specific to the protracted speciation model, involves a flattening of the species abundance distribution at low abundances (e.g.,  $m = 0.1$ ,  $\theta = 4$ ,  $J = 10^4$  in Fig. S1C). This effect is too small to see clearly for the range of parameter values shown in Fig. S1, but is somewhat more pronounced in very large communities with very low values of the biodiversity parameter ( $\theta \sim 1$ ), for which the ratio of individuals to species is very high (e.g., a local community with 10,000 individuals but only about 10 species). The third class of cases are specific to the fission speciation model and involve an excess of rare species, relative to the Poisson-gamma distribution (e.g.,  $m = 0.01$ ,  $J = 10^4$ ,  $\theta = 40$  in Fig. S1D). As with the second class of cases, this effect is relatively small in Fig. S1, but can be more pronounced for very large, particularly isolated, communities with few species (e.g., 10,000 individuals and about 10 species, implying mean abundances of about 1,000). For the data analyzed in this paper,

however, most sites are very far from these extreme low-diversity cases. The typical (median) site is a sample of 422 individuals containing 17 species, and very few sites contain so few species at such large sample sizes (86% of sites, for instance, have mean species abundances of 100 or less). Moreover, the individual datasets vary substantially in community size and observed species richness (e.g., mean site richness varies from 9 to 126 species across the 14 datasets, and average species abundances at the site level range from 4 to 123 across all datasets except one). Thus, the overwhelming majority of our sites could not correspond to those regions of parameter space where the Poisson-gamma distribution performs less well as an approximation for neutral dynamics.

**Robustness to Ecological and Taxonomic Heterogeneity.** Although neutral models have previously been applied to very heterogeneous communities (19), including benthic marine invertebrates (2) [and indeed their capacity to characterize such systems has been invoked as evidence of their robustness (2)], most neutral model communities are conceptualized as a guild of organisms competing for a shared set of resources. Some of our datasets are relatively taxonomically and ecologically homogeneous [e.g., Indo-Pacific Coral Crustaceans (IPC), which contains only crustaceans associated with dead coral heads]. However, others are more heterogeneous. Therefore, to determine whether our results were sensitive to this taxonomic and ecological heterogeneity of the assemblages, we classified our species into guilds, where information was available, and reanalyzed our species abundance data, limiting the analysis to species from the most species-rich guild for each dataset (Table S3). Such a classification is necessarily approximate for marine animals, given the high degree of omnivory in the ocean. Nevertheless, the analysis allows us to evaluate whether or not our conclusions are sensitive to the extent of heterogeneity in the data. The resolution of the groupings for this analysis depended somewhat on both the taxonomic and ecological heterogeneity of the original data, and also on the species richness in the samples. Specifically, we used as a rule of thumb that guilds should have a minimum of 10 species, necessitating use of more coarse groupings for more species-poor datasets.

By restricting the analysis to a subset of the species, the statistical power to detect differences between Poisson-lognormal and Poisson-gamma species abundances is reduced—the more heterogeneous the original dataset, the smaller the subset of species that could be included in the analysis. Nevertheless, strong support for the Poisson-lognormal remained: across site, mesoscale, and regional levels, the Poisson-lognormal was strongly (>95%) supported in 27 cases, whereas the Poisson-gamma was strongly supported in only 1 (Table S3).

**Analysis of Variation in the Shapes of Species Abundance Distributions.** Standardizing model support by dividing by the number of observed species abundances successfully controlled for the effects of statistical power shown in Fig. 2, at least at the site level and mesoscale: mixed-effects linear model analyses using the number of distinct species abundance values as an explanatory variable indicated that the overall effect did not differ significantly from zero, and explained about 1–10% of the variation in standardized model support across datasets (see  $R^2$  values in Table S4). In contrast, the strength of support for the Poisson-lognormal over the Poisson-gamma increased strongly with the relative abundance of the most abundant species at site, mesoscale, and regional (whole-dataset) levels. The positive relationship was highly consistent between datasets at both the site level and mesoscale (gray lines in Fig. S4 A and C), and explained about one-half or more of the variation (Table S4 and Fig. S4 B, D, and E). In contrast, the proportion of singletons was a poor predictor of relative model performance: the estimated direction of the effect was not con-

sistent across datasets at the site level (gray lines in Fig. S5A), and the estimated overall effect did not differ significantly from zero at any scale (Table S4 and black lines in Fig. S5 A, C, and E) and never explained more than 16% of the variation (Table S4).

To further assess the strength of these results, we repeated our common-species analysis using the combined relative abundance of the three most abundant species. This, too, was strongly positively related to support for the Poisson-lognormal distribution (slope:  $0.40 \pm 0.02$ , pseudo- $R^2 = 0.44$  at site level;  $0.24 \pm 0.05$ ,

pseudo- $R^2 = 0.53$  at mesoscale level;  $0.15 \pm 0.04$ ,  $R^2 = 0.55$  at regional scale). Conversely, expanding our definition of rarity to encompass the proportion of species in the bottom two octaves (species with abundance 3 or less) did not improve its effectiveness as a predictor of standardized support for the Poisson-lognormal over the Poisson-gamma: the overall relationship did not differ significantly from zero at any scale (no slopes significantly different from zero, pseudo- $R^2 < 0.02$  at site-scale and mesoscale levels,  $R^2 = 0.21$  at regional level).

1. Pueyo S (2006) Diversity: Between neutrality and structure. *Oikos* 112(2):392–405.
2. Hubbell SP (2001) *The Unified Neutral Theory of Biodiversity and Biogeography* (Princeton Univ Press, Princeton).
3. Volkov I, Banavar JR, Hubbell SP, Maritan A (2007) Patterns of relative species abundance in rainforests and coral reefs. *Nature* 450(7166):45–49.
4. Rosindell J, Cornell SJ (2013) Universal scaling of species-abundance distributions across multiple scales. *Oikos* 122(7):1101–1111.
5. Etienne R, Haegeman B (2011) The neutral theory of biodiversity with random fission speciation. *Theor Ecol* 4(1):87–109.
6. Pielou EC (1977) *Mathematical Ecology* (Wiley, New York).
7. Connolly SR, Dornelas M, Bellwood DR, Hughes TP (2009) Testing species abundance models: A new bootstrap approach applied to Indo-Pacific coral reefs. *Ecology* 90(11): 3138–3149.
8. Sæther BE, Engen S, Grøtan V (2013) Species diversity and community similarity in fluctuating environments: Parametric approaches using species abundance distributions. *J Anim Ecol* 82(4):721–738.
9. Etienne RS, Alonso D (2005) A dispersal-limited sampling theory for species and alleles. *Ecol Lett* 8(11):1147–1156.
10. Rosindell J, Cornell SJ, Hubbell SP, Etienne RS (2010) Protracted speciation revitalizes the neutral theory of biodiversity. *Ecol Lett* 13(6):716–727.
11. He F (2005) Deriving a neutral model of species abundance from fundamental mechanisms of population dynamics. *Funct Ecol* 19(1):187–193.
12. Volkov I, Banavar JR, He FL, Hubbell SP, Maritan A (2005) Density dependence explains tree species abundance and diversity in tropical forests. *Nature* 438(7068): 658–661.
13. Allen AP, Savage VM (2007) Setting the absolute tempo of biodiversity dynamics. *Ecol Lett* 10(7):637–646.
14. Ostling A (2012) Do fitness-equalizing tradeoffs lead to neutral communities? *Theor Ecol* 5(2):181–194.
15. Burnham KP, Anderson DR (2002) *Model Selection and Multi-Model Inference: A Practical Information-Theoretic Approach* (Springer, Heidelberg).
16. Connolly SR, Hughes TP, Bellwood DR, Karlson RH (2005) Community structure of corals and reef fishes at multiple scales. *Science* 309(5739):1363–1365.
17. McQuarrie ADR, Tsai C-L (1998) *Regression and Time Series Model Selection* (World Scientific, River Edge, NJ).
18. Burnham KP, Overton WS (1979) Robust estimation of population size when capture probabilities vary among animals. *Ecology* 60(5):927–936.
19. de Aguiar MAM, Baranger M, Baptestini EM, Kaufman L, Bar-Yam Y (2009) Global patterns of speciation and diversity. *Nature* 460(7253):384–387.

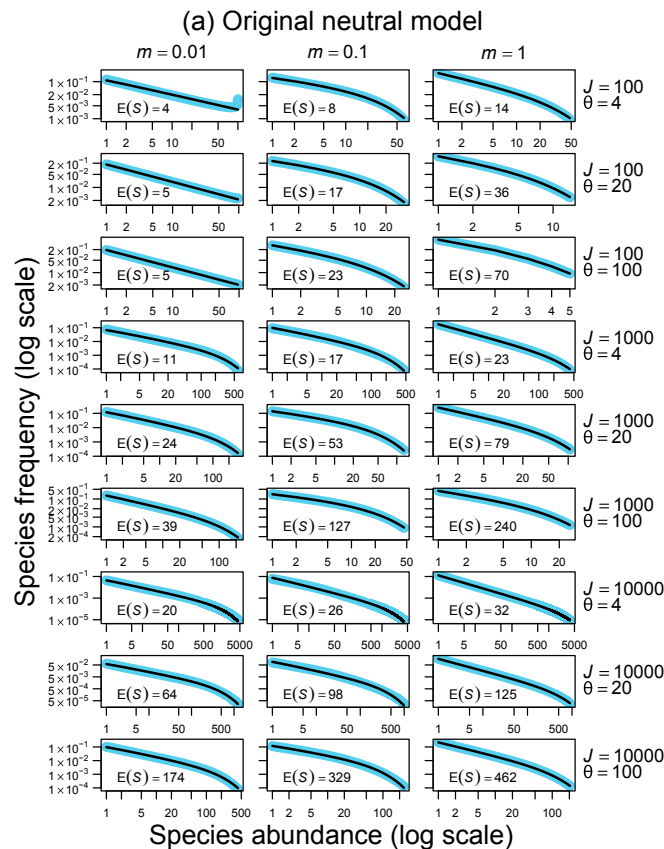
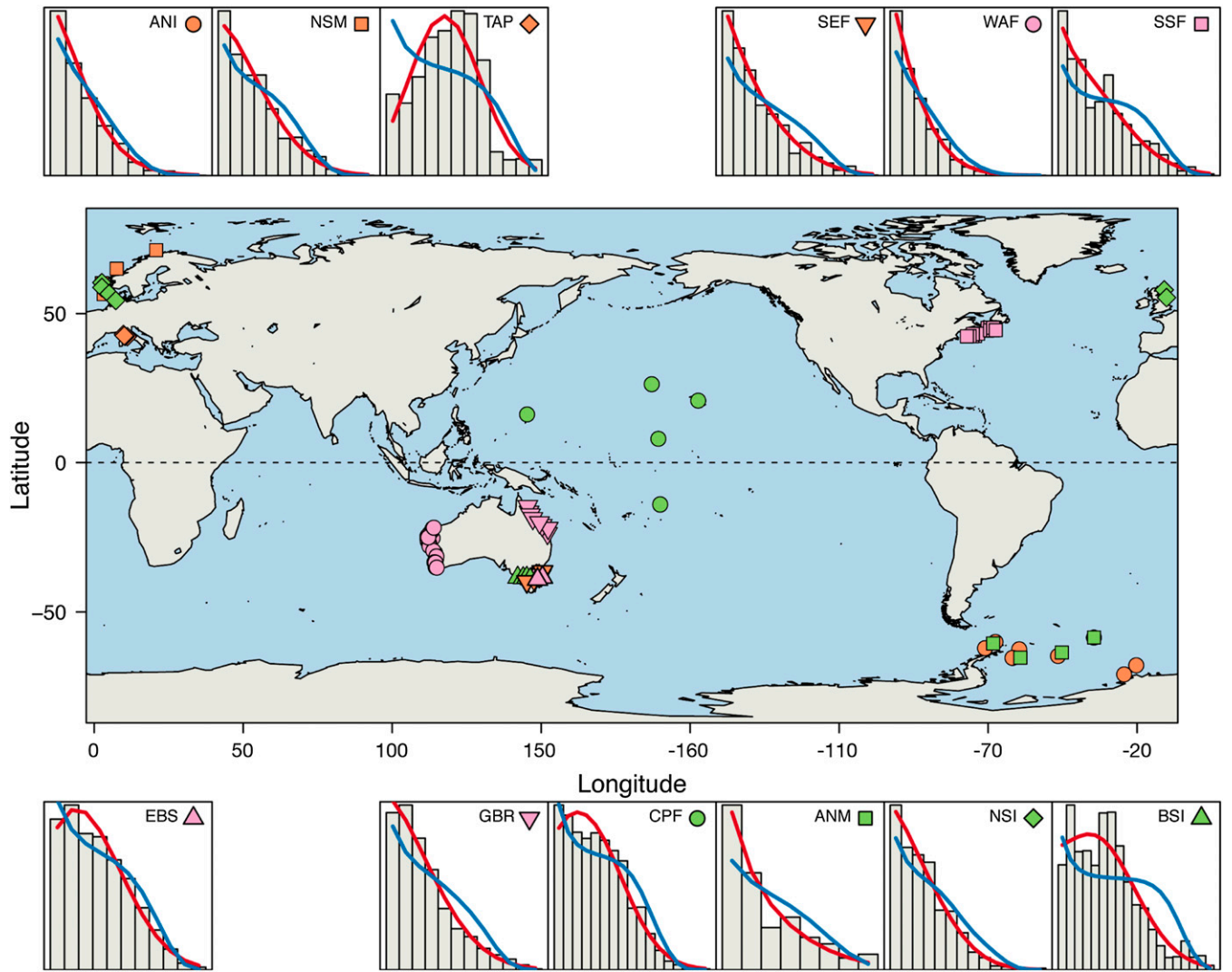


Fig. S1. (Continued)







**Fig. S2.** Observed and best-fit mesoscale abundance distributions. On the map, different combinations of colors and symbols correspond to different datasets: these are reproduced in the corresponding figure panels. See Table S1 for metadata, including abbreviations. Each point on the map is located at the centroid of the individual sites that were pooled to generate each mesoscale abundance distribution. Panels above and below the map compare observed and fitted species abundance distributions at this scale. The bars represent the mean proportion of species in different octave classes of abundance, across all mesoscale abundance distributions from the corresponding ecosystem (these are shown as true doubling classes: the first bar represents species with abundance 1; the second, abundances 2–3; the third, abundances 4–7; etc.). The blue and red lines show the mean of fitted values from fits of the Poisson-gamma and Poisson-lognormal distributions, respectively, to each mesoscale abundance distribution.



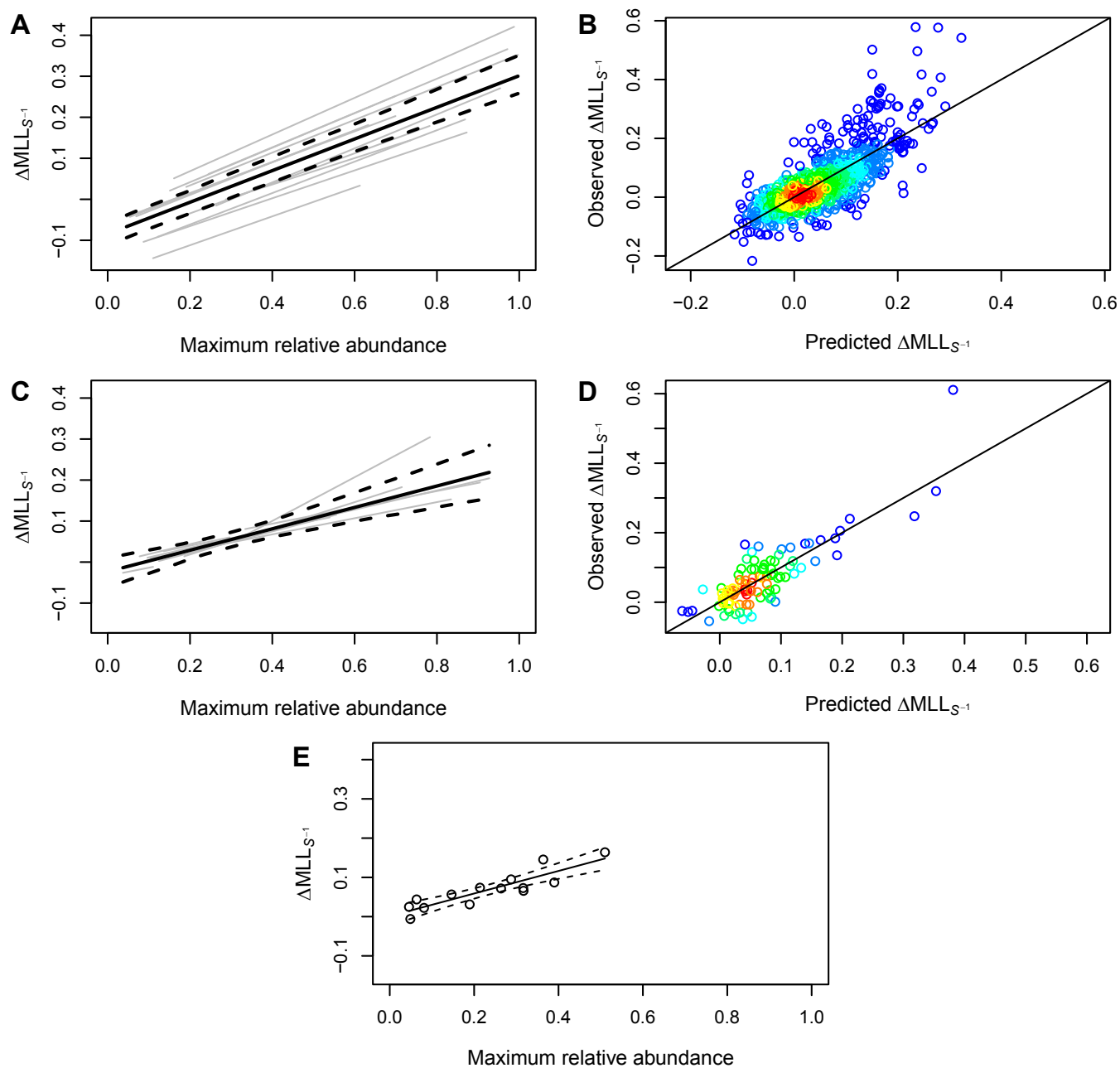


**Fig. 54.** Analysis of the variation in standardized support for the lognormal explained by the relative abundance of the most-abundant species (expressed as a fraction of the number of individuals sampled), at the (A and B) site scale, (C and D) mesoscale, and (E) regional scale. Positive relationships indicate stronger evidence against the gamma neutral approximation as the most-abundant species becomes more dominant. In A and C, the thick solid and dashed lines represent the overall (i.e., fixed effects) relationship, with 95% confidence intervals. The gray lines represent the relationships for the 14 individual datasets, based on the estimated random effects; individual lines are drawn to span only the range of horizontal axis values observed in the corresponding dataset. B and D show corresponding plots of observed versus predicted values, as estimated from the full fitted model. Because there is substantial overlap of points, the points have been color-coded according to the number of nearby observations, grading from red (high density of points) to blue. E is an ordinary least-squares (OLS) regression: because there is only one (pooled) regional abundance distribution per site, there is no random effect.









**Table S3. Groupings used and model selection for single-guild analysis**

Dataset	Guild name	No. of species in group	% of sites fitted at site level	% support for lognormal		
				Site	Mesoscale	Regional
Antarctic Isopods (ANI)	Detritus feeders	486	82	> <b>0.9999</b>	> <b>0.9999</b>	> <b>0.9999</b>
Antarctic Molluscs (ANM)	Suspension feeders	24	0	NA	0.7048	0.8639
Tuscany Archipelago Fish (TAP)	Benthic feeders	38	100	> <b>0.9999</b>	<b>0.9999</b>	<b>0.9973</b>
Indo-Pacific Coral Crustaceans (IPC)	Decapods	334	100	> <b>0.9999</b>	NA	> <b>0.9999</b>
SE Australia: Shelf Fish (SEF)	Invertivores, benthic prey	101	57	> <b>0.9999</b>	<b>0.9999</b>	0.8741
W Australia: Deep Fish (WAF)	Invertivores, benthic prey	121	38	<u>0.0199</u>	> <b>0.9999</b>	<b>0.9958</b>
Scotian Shelf Fish (SSF)	Invertivores	48	6	<u>0.0727</u>	> <b>0.9999</b>	<b>0.9998</b>
Eastern Bass Strait Invertebrates (EBS)	Deposit feeders	347	91	> <b>0.9999</b>	> <b>0.9999</b>	0.2905
Sunderban Zooplankton (SUZ)	Planktivores	27	100	> <b>0.9999</b>	NA	<b>0.9772</b>
Great Barrier Reef Fish (GBR)	Herbivores	60	53	> <b>0.9999</b>	> <b>0.9999</b>	<b>0.9515</b>
Central Pacific Reef Fish (CPF)	Invertivores	164	100	> <b>0.9999</b>	<b>0.9998</b>	0.8776
Norwegian Shelf Macrobenthos (NSM)	Deposit feeders, Malacostraca only	76	4	0.6079	<b>0.9902</b>	0.7062
North Sea Invertebrates (NSI)	Deposit feeders	74	74	0.6953	0.0902	0.0593
Bass Strait Intertidal (BSI)	Grazers	49	100	> <b>0.9999</b>	> <b>0.9999</b>	<b>0.9937</b>
Overall				> <b>0.9999</b>	> <b>0.9999</b>	> <b>0.9999</b>

Percentage support values indicate relative support for the Poisson-lognormal over Poisson-gamma model fitted to the species abundance data at three scales: site level, mesoscale, and regional. Each row represents a different dataset. For ANM, there were no sites with more than five distinct species abundance values for the most species-rich functional group, so model selection was only done at the mesoscale and regional scale. For IPC and SUZ, there were too few species abundance distributions to create mesoscale groupings. The last row is an overall test, based on summing the log-likelihoods across all datasets. Where lognormal model has at least 95% support, the model's weight is shown in bold. Where Poisson-gamma model has at least 95% support, the model's weight is shown underlined.

**Table S4. Mixed-effects and OLS regression model results for analysis of standardized relative support for the Poisson-lognormal**

Explanatory variable	Overall slope <sup>†</sup> ± SE	t <sup>‡</sup>	Marginal R <sup>2</sup> §	Pseudo-R <sup>2</sup>	AIC
<b>Site level</b>					
Intercept only	NA	NA	0.00	0.08	-1,879.6
Log(no. of distinct abundances)	-0.009 ± 0.015	-0.58	<0.01	0.11	-1,883.2
Maximum relative abundance	0.386 ± 0.020	19.66***	0.47	0.60	-2,641.5
Proportion of singletons	0.074 ± 0.051	1.45	0.01	0.14	-1,913.6
<b>Mesoscale</b>					
Intercept only	NA	NA	0.00	0.00	-186.4
Log(no. of distinct abundances)	-0.009 ± 0.013	-0.74	0.01	0.01	-181.0
Maximum relative abundance	0.261 ± 0.051	5.08***	0.24	0.71	-270.8
Proportion of singletons	0.046 ± 0.074	0.63	<0.01	<0.01	-180.8
<b>Regional</b>					
	Slope ± SE	t		R <sup>2</sup>	AIC
Intercept only	NA	NA		0.00	-43.3
Log(no. of distinct abundances)	-0.039 ± 0.014	-2.83*		0.40	-48.5
Maximum relative abundance	0.288 ± 0.043	6.75***		0.79	-63.3
Proportion of singletons	-0.160 ± 0.108	-1.48		0.16	-43.7

Except for Akaike's information criterion (AIC), which was calculated from maximum-likelihood fits, all values reported in the table were obtained using restricted maximum likelihood (REML).

<sup>†</sup>"Overall slope" refers to the fixed effects component of the model.

<sup>‡</sup>The t statistic for the slope parameter. The number of asterisks indicates the level of statistical significance:

\*0.01 < P < 0.05, \*\*0.001 < P < 0.01, and \*\*\*P < 0.001.

<sup>§</sup>Percentage of variation explained by the fixed effect only.

<sup>¶</sup>Calculated from the residuals of the full fitted model ( $1 - (\sigma_{resid}^2 / \sigma_{tot}^2)$ ).